

JET-P(92)17

B.E. Keen, M.L. Watkins  
and JET Team

# The New Phase of JET: The Pumped Divertor

“This document contains JET information in a form not yet suitable for publication. The report has been prepared primarily for discussion and information within the JET Project and the Associations. It must not be quoted in publications or in Abstract Journals. External distribution requires approval from the Publications Officer, JET Joint Undertaking, Abingdon, Oxon, OX14 3EA, UK”.

“Enquiries about Copyright and reproduction should be addressed to the Publications Officer, EFDA, Culham Science Centre, Abingdon, Oxon, OX14 3DB, UK.”

The contents of this preprint and all other JET EFDA Preprints and Conference Papers are available to view online free at [www.iop.org/Jet](http://www.iop.org/Jet). This site has full search facilities and e-mail alert options. The diagrams contained within the PDFs on this site are hyperlinked from the year 1996 onwards.

# The New Phase of JET: The Pumped Divertor

B.E. Keen, M.L. Watkins  
and JET Team\*

*JET-Joint Undertaking, Culham Science Centre, OX14 3DB, Abingdon, UK*

*\* See Annex*

Preprint of Paper to be submitted for publication in  
Europhysics News



# THE NEW PHASE OF JET: THE PUMPED DIVERTOR

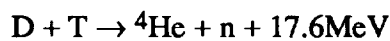
B.E. KEEN AND M.L. WATKINS

AND THE JET TEAM

JET Joint Undertaking, Abingdon, Oxon, U.K.

## INTRODUCTION

The basic principle of the fusion process is the fusing of light nuclei to form heavier ones and the accompanying release of substantial energy. For a fusion reactor, there are several possible fusion reactions, but the one that is easiest to achieve is that between the deuterium and tritium isotopes of hydrogen. This D-T reaction is:



At the temperatures needed for this reaction to occur, the D-T fuel is in the plasma state, comprising a mixture of charged particles (nuclei and electrons), which can be contained by magnetic fields. The most effective magnetic configuration is the toroidal tokamak device, of which the Joint European Torus (JET) is the largest in operation.

For a D-T fusion reactor, the triple fusion product of the temperature ( $T_i$ ), density ( $n_i$ ) and energy confinement time ( $\tau_E$ ) must exceed the value ( $n_i \cdot \tau_E \cdot T_i$ ) of  $5 \times 10^{21} \text{m}^{-3} \text{skeV}$ . This measures the performance of a fusion device and shows how close conditions are to those of a reactor. Typically, for a reactor based on magnetic confinement concepts, the following are required:

Central ion temperature, $T_i$	10-20keV
Central ion density, $n_i$	$2.5 \times 10^{20} \text{m}^{-3}$
Global energy confinement time, $\tau_E$	1 - 2s

During the early 1970's, it was clear that the achievement of near-reactor conditions required much larger experiments, which were likely to be beyond the resources of any individual country. In 1973, it was decided in Europe that a large device, the Joint European Torus (JET), should be built as a joint venture (see Fig.1). The formal organization of the Project - the JET Joint Undertaking - was set up near Abingdon, U.K., in 1978. The Project Team is drawn from Euratom and the fourteen member nations - the twelve EC countries, together with Switzerland and Sweden. By mid-1983, the construction of JET, its power supplies and buildings were completed on schedule and broadly to budget and the research programme started.

JET is the largest project in the coordinated programme of EURATOM, whose fusion programme is designed to lead ultimately to the construction of an energy producing reactor.

Its strategy is based on the sequential construction of major apparatus such as JET, a Next Step device and a demonstration reactor (which should be a full ignition, high power device), supported by medium sized specialized tokamaks.

The objective of JET is to obtain and study a plasma in conditions and dimensions approaching those needed in a thermonuclear reactor [1,2]. This involves four main areas of work:

- (i) to study various methods of heating plasmas to the thermonuclear regime;
- (ii) to study the scaling of plasma behaviour as parameters approach the reactor range;
- (iii) to study the interaction of plasma with the vessel walls and how to continuously fuel and exhaust the plasma;
- (iv) to study the production of alpha-particles generated in the fusion of deuterium and tritium atoms and the consequent heating of plasma by these alpha-particles.

The first and second areas of work have now been well covered and the third area of work has been well studied in the limiter configuration for which JET was originally designed. However, the highest performance JET discharges have been obtained with a "magnetic limiter", that is, in the so-called "X-point configuration" with a magnetic separatrix inside the vacuum vessel, with plasma contacting localised areas of wall (the X-point targets) and detached from the limiters except during the formation of the discharge. The duration of the high performance phase of these discharges can exceed 1.5s by careful design of the targets and specific operational techniques, but is limited, ultimately, by an unacceptably high influx of impurities. The fourth area of work had been started by earlier studies of energetic particles produced as fusion products or by ion cyclotron resonance heating (ICRH). It has now been addressed further by the first tokamak plasma experiments in deuterium-tritium mixtures. These results are presented briefly in the following sections.

## **PLASMA PERFORMANCE AND IMPURITY CONTROL**

JET is now in the second half of its experimental programme. The technical design specifications of JET have been achieved in all parameters and exceeded in several cases (see Table I). The plasma current of 7MA and the current duration of up to 60s are world records and are more than twice the values achieved in any other fusion experiment. The neutral beam injection (NBI) heating system has been brought up to full power (~21MW) and the ion cyclotron resonance frequency (ICRF) heating power has been increased to ~20MW in the plasma. In combination, these heating systems have provided over 35MW of power to the plasma.

Since the start of operation in 1983 the study of plasma-wall interactions under such high power conditions and the control of impurities have always been considered as key scientific

and technical issues to which particular attention has been paid. Impurity production has been reduced by both **passive** methods of impurity control (such as the proper choice of plasma-facing components - beryllium or beryllium carbide) and **active** methods of impurity control (such as sweeping the magnetic configuration, and hence the plasma, across the targets at which the plasma-wall interaction is often localised). The resulting significant improvements in plasma performance have brought JET to near "breakeven" conditions and to within a factor of 5 of the fusion triple product needed for a fusion reactor.

Up to 1988, JET operated with a carbon first wall (carbon tiles and wall carbonisation). A fusion triple product ( $n_D T_i \tau_E$ ) of  $2.5 \times 10^{20} \text{m}^{-3} \text{keVs}$  was achieved [3]. The attainment of higher plasma parameters was limited by impurity influxes, mostly carbon and oxygen, from the walls. The impurities diluted the plasma fuel, thereby decreasing the fusion reactivity and increasing the radiative energy losses. Excessively high impurity influxes (called the "carbon bloom") were observed during high power heating and led to a rapid deterioration of plasma parameters and fusion performance [4].

From 1989, JET has operated with a beryllium first wall. Because of its low atomic number, beryllium was expected to lead to superior plasma performance, resulting in much reduced radiative losses compared with carbon. It also has the advantage of acting as a getter for oxygen [5]. The experimental campaigns of 1989 and 1990 confirmed these expectations. The chief effect of beryllium is to improve plasma purity (defined as the ratio of fuel ion to electron densities) and, as a result, to increase plasma performance. A fusion triple product ( $n_D T_i \tau_E$ ) of  $8-9 \times 10^{20} \text{m}^{-3} \text{keVs}$  was achieved at both high ion temperatures ( $>20 \text{keV}$ ) (the so-called "hot ion mode"), and medium temperatures ( $9 \text{keV}$ ), in the parameter range that is more relevant to fusion reactors. The details of these physics results and fusion relevant parameters have been reported previously [6].

Towards the end of 1991, the performance of JET plasmas had improved sufficiently to warrant the first tokamak experiments using a deuterium-tritium (D-T) fuel mixture. Tritium neutral beams were injected into a deuterium plasma, heated by deuterium neutral beams. This introduced up to 10% of tritium into the machine, although ultimately about 50% tritium will be used in a reactor. As a consequence, a significant amount of power was obtained in JET from controlled nuclear fusion reactions. The peak fusion power generated reached about 1.7MW in a pulse lasting for 2 seconds, giving a total energy release of 2MJ. This was clearly a major step forward in the development of fusion as a new source of energy, and should permit extrapolation to a Next Step device, which should demonstrate ignition in a routine way.

However, as in all high performance discharges, the high power phase is transient, lasting for less than 1s. It could not be sustained in the steady state: the impurity influx observed with

carbon walls also occurs with beryllium and causes a degradation of plasma parameters. This emphasises the need for improved methods of impurity control in fusion devices.

## **THE NEW PHASE OF JET AND THE PUMPED DIVERTOR**

The aim of the New Phase is to demonstrate, prior to full D-T operation in JET, effective methods of impurity control in operating conditions close to those of a Next Step tokamak, with a stationary plasma of 'thermonuclear grade' in an axisymmetric pumped divertor configuration. The New Phase should demonstrate a concept of impurity control; determine the size and geometry needed to realise this concept in a Next-Step tokamak; allow a choice of suitable plasma facing components; and demonstrate the operational domain for such a device. The New Phase for JET starts in 1992 [5], with first results becoming available in 1993; the programme will then continue to the end of 1996.

The divertor configuration channels particle and energy flows along the open magnetic field lines just outside the separatrix from the main plasma towards a localised, remote target and pumping region (Fig.2). Impurity production is minimised by the proper selection of target materials and by reducing the plasma temperature at the targets as far as possible. Although the principal source of impurities is well removed from the main plasma, sputtered impurities cannot be eliminated completely and these have then to be retained in the divertor region in order to avoid contaminating the main plasma. In principle, this can be achieved by a strong flow of deuterium directed towards the targets, preventing the back diffusion of impurities under the influence of frictional forces. The X-point should be well separated from the targets, allowing a long connection length (~5-10m) along the open magnetic field lines, between the X-point region and the targets. This allows the plasma temperature near the targets to fall to acceptable levels and the effective screening of impurities to occur.

The general features of the JET pumped divertor are illustrated in Fig.2. It is of the "open" type, with beryllium-clad, water cooled (Hypervapotron) copper target plates. The in-vessel four-coil system allows both for horizontal sweeping of the plasma along the target to spread the heat load, and for vertical motion of the magnetic X-point to vary the connection length and plasma volume. The possible divertor configurations span the range from a "slim" 5MA plasma (total divertor coil current of 1.8MA) with the connection length of about 8.2m, to a "fat" 6MA plasma with a connection length 3.1m (see Table II).

## **A CONCEPT FOR IMPURITY CONTROL**

The key concept of the JET pumped divertor, namely the retention of impurities near the targets by inducing a strongly directed flow of plasma particles along the divertor channel towards the



targets, is now discussed in more detail. Impurities produced at the targets are subject to several forces, as given by the steady-state momentum equation:

$$m_z n_z v_z \frac{dv_z}{dx} = -\frac{dp_z}{dx} + Zen_z E + \frac{m_z n_z (v_i - v_z)}{\tau_{zi}} + n_z \alpha_z \frac{dT_e}{dx} + n_z \beta_z \frac{dT_i}{dx} \quad (1)$$

Here we have considered a single impurity species of charge state  $Z$ , mass  $m_z$ , density  $n_z$ , temperature  $T_z$ , pressure  $p_z$ , and flow speed  $v_z$  along the field (coordinates). The most important forces are the ion thermal force, directed away from the targets, the deuterium-impurity friction force directed towards the targets, and the impurity pressure gradient force which arises to establish a force balance. The electric field may be eliminated from this equation by using the electron momentum equation and taking the electron pressure to be nearly constant along  $s$ . Eq.(1) then becomes:

$$\frac{T_i}{n_z} \frac{dn_z}{ds} = \frac{m_z (v_i - v_z)}{\tau_{zi}} + (\alpha_z - 0.71Z) \frac{dT_e}{ds} + (\beta_z - 1) \frac{dT_i}{ds} \quad (2)$$

For most cases of interest,  $\nabla T_e \ll \nabla T_i$ , since they are both determined by classical heat conduction and  $\kappa_{//e} \gg \kappa_{//i}$ . The ion thermal force (the last term on the right side of Eq.(1)) is then dominant and is determined principally by the ion heat flow into the scrape-off layer (SOL). The counter-acting frictional force (the first term on the right side of Eq.(2)) depends on the magnitude and spatial distribution of the deuterium particle flux,  $nv_i$ , and is proportional to  $(1/T_i^{3/2})$ , where  $T_i$  is the ion temperature. Thus, in principle, the friction force can be set at a level sufficient to overcome the thermal force.

At high scrape-off layer densities, large plasma flows near the targets are established naturally by the ionization of neutrals that recycle at the targets. This ensures impurity control within an effective ionization length at the target, with the plasma flows increasing rapidly on approaching the target. Some neutrals, however, are not recycled locally near the targets, but escape and re-enter the scrape-off layer nearer the X-point after reflection from the torus walls, or transmission across the private flux region. This "distant recycling" then extends the region of significant plasma flow, and the effectiveness of the friction force term further from the targets. It is also possible, in principle, to increase "distant recycling" by extracting some of the plasma flow at the targets and directly "recirculating" the flow as neutrals, into the X-point region. Baffles might be needed to facilitate this. At lower scrape-off layer densities, the natural flow from the main plasma is not amplified sufficiently by recycling at the targets to ensure impurity retention. Strong gas puffing or shallow pellet injection into the scrape-off layer is needed. Steady state operation with such "external recirculation" then requires the pumping of an equivalent neutral flux from the divertor chamber and this can impose severe pumping requirements.

Another important feature of the pumped divertor is the formation of a cold and dense target plasma in the divertor channels. The cold dense plasma in front of the targets is expected:

- to radiate a significant fraction of the plasma input power, thus reducing the heat load on the targets;
- to reduce the impurity production by shielding the targets;
- to reduce the probability of impurities returning to the plasma.

## **TECHNICAL ASPECTS**

### **(a) Magnetic Configuration**

The configuration features four divertor coils as shown in Fig.3. Figs. 4 and 5 show the plasma configurations which can be achieved. This number of coils reflects the experimental nature of the JET pumped divertor programme, and the need for operational flexibility. The four coils will allow exploration of a wide range of magnetic configurations. All four coils carry currents in the same direction. The two bottom central coils produce the X-point and have been made as flat as possible to increase the volume available to the plasma. The two side coils allow a reduction of the poloidal field in the region between the X-point and the target plates, thus changing the pitch of the magnetic field lines and consequently increasing the connection length. Since all four coils will have independent power supplies, greater flexibility can be achieved in the type of magnetic configuration as shown on Figs.4 and 5 and in Table II.

The side coils allow the connection length to be adjusted both independently of the plasma current and separately on the inboard and outboard sides of the X-point. The strike zone of the separatrix and scrape-off layer can be swept radially to reduce the power deposition to an acceptable time average value. A total sweep amplitude of 20cm at a frequency of 4Hz is possible without significant changes of the connection length both inboard or outboard.

The coils are conventional and use water cooled copper conductors. They will be assembled inside the vessel from preformed one-third turn segments. The coils include 15 to 21 turns and carry typically 0.6MA turns. The divertor configuration can be maintained for typically 10s at 6MA, and up to one minute at 2MA.

### **(b) Target Plates**

The targets feature three elements (see Fig.6) in a U-configuration to accommodate the plasma and divertor contours. Horizontal plates at the bottom intersect the heat flux conducted along field lines. Therefore, these bottom targets are subjected to a severe power deposition. Vertical targets on either side intersect the power radiated from the divertor plasma and receive only a modest heat load. The horizontal and vertical targets are split into 384 radial elements grouped into 48 modules of eight elements each.

In this configuration, the peak power density on the bottom targets would be unacceptably high even for the most advanced heat sinks. Consequently, sweeping the magnetic field across the targets is essential. The load can be accommodated by hypervaportrons of the type used on the JET neutral beam systems. In contrast to the bottom targets, the side targets receive only modest radiative heat load from the divertor plasma.

The surface of the hypervaportrons facing the plasma must be clad with a low-Z material. The choice of beryllium is natural in view of the results already achieved on JET, although it is recognised that beryllium impurities generated in the divertor plasma will radiate only a negligible fraction of the incident power. However, the choice of material other than beryllium would entail the risk of impurities migrating back to the plasma and jeopardising the benefits of a beryllium first wall. Installation of the targets will proceed in two steps. During 1993, Mark I will use solid radiatively cooled beryllium blocks as targets. In 1994, Mark II will use water-cooled beryllium clad hypervaportrons. This approach was motivated by the desire to start pumped divertor operation with a robust and simple design.

### **(c) The Cryopump**

In the JET divertor, pumping will be achieved partly by the beryllium target plates and partly by a cryopump. Pumping by beryllium surfaces has been observed to diminish and stop during long pulses (>30 seconds) and the cryopump is expected to play an essential role particularly for long pulse experiments. A cryopump, rather than a getter or titanium sublimation pump, has been selected because it has no tritium inventory after regeneration, it is not affected by plasma operation or clean up techniques (glow discharge).

A drawback of the cryopump is its sensitivity to thermal loads. Pumping takes place through gaps between the target elements and is seriously restricted by the need to protect the helium cooled surfaces from high temperature gas molecules and thermal radiation. The design uses a liquid nitrogen cooled chevron baffle and water cooled structures.

Nuclear heating is expected to be the most severe heat load. In the case of operation at breakeven with a neutron production of  $10^{19}\text{s}^{-1}$ , power of 4.5kW is expected to be absorbed by the helium and the stainless steel helium conduits. To minimise nuclear heating, the conduits have thin walls and are slightly corrugated for increased strength. The heat capacity of the helium content of the pump ( $\sim 40$  litres) is about 50kJ for a 1K temperature rise and should limit the pulse duration only if operation close to breakeven is achieved.

The pump has a nominal pumping speed for deuterium at 300K of  $5 \times 10^5 \text{ l s}^{-1}$  and has the thermal capacity to cope with up to  $10^{23}$  particles per second. The actual pumping efficiency

depends crucially on the parameters of the divertor plasma, which should ideally be cold and dense, and on the neutral gas pressure in the vicinity of the target plates. The pump is split into quadrants in the toroidal direction and will have two cryo-supplies each common to two quadrants. The details are shown in Fig.7.

#### **(d) Fuelling**

Pellet fuelling is expected to play a key role in controlling the plasma density profile and impurity and alpha-particle concentrations in the plasma. Fast pellets at velocities up to  $4\text{kms}^{-1}$  are planned to fuel the plasma centre and flush impurities towards the edge. Fast pneumatic guns, under development at JET, are expected to be available for divertor operation.

Low velocity pellets (up to  $500\text{ms}^{-1}$ ) launched by a centrifugal injector can fuel the outermost layers of the plasma and enhance the flow of plasma towards the targets. This type of gun should have the capability to deliver long strings of small pellets ( $27\text{mm}^3$ ,  $40\text{s}^{-1}$  for 10-30s) and is being built at JET. Gas puffing will also be used, if required, to enhance recycling in the vicinity of the targets. Twenty-four gas nozzles distributed along the torus will inject gas inside the triangular region formed by the magnetic separatrix and targets.

#### **(e) Other Components of the Divertor Configuration**

Eight Ion Cyclotron Resonance Heating (ICRH) antennae will be used to heat the plasma. Each antennae is designed to be moved radially and tilted to match the plasma shape and maximise power coupling.

Twelve discrete poloidal rail limiters are also provided for plasma start up and to protect the ICRH antennae. These limiters are large vertical structures attached to the outboard wall of the vacuum vessel and similarly to the antennae, they can be moved radially and tilted. These limiters will carry radiation cooled beryllium tiles on their front face. The inboard wall protections are carbon fibre composite (CFC) tiles mounted on rigid vertical beams attached to the inboard wall reinforcing rings.

#### **(f) Diagnostics**

In view of the experimental nature of the pumped divertor, an extensive range of diagnostics is planned. Many of these diagnostics are an integral part of the target assemblies. The full list is shown in Table III.

The main measurement goals are the local magnetic geometry near the targets (flux loops and magnetic probes), the plasma temperature and density in the divertor (Langmuir probes,

LIDAR Thomson scattering, microwave systems including interferometry, reflectometry and electron cyclotron absorption), impurity behaviour in the divertor (VUV and visible spectroscopy), the radiated power in the divertor channels (bolometer array), and the neutral gas pressure near the targets (pressure probes).

The targets and cooling pipes will be fitted with thermocouples which will yield data on temperature distributions and total incident power. Thermographic observation of the target plates using CCD cameras with infra-red filters is also foreseen.

## **EXPERIMENTAL PROGRAMME**

Installation is planned to start early in 1992 and should take ~18 months. The programme with the pumped divertor is split into two periods (see Table IV). The first operation period will use the Mark I targets (radiation cooled) and will focus on establishing reliable operation, defining parameter space, and identifying the optimum magnetic configuration.

A short shutdown will then allow for replacement of Mark I with Mark II targets (water cooled) and for installation of the ICRH antennae and the outboard limiters in the positions which match the chosen plasma configuration. Other minor modifications may also be carried out at this stage. The second period of operation will be devoted to the study of impurity control at high power and during longer pulses.

## **CONCLUSIONS**

Individually, each of the plasma parameters  $n$ ,  $T_i$  and  $\tau_E$  required for a fusion reactor have been achieved in JET; in single discharges. The triple fusion product of these parameters has now reached equivalent break-even conditions and is within a factor five of that required in a fusion reactor. However, these good results were obtained only transiently, and were limited by impurity influxes due to local overheating of protection tiles. These experimental results emphasize the importance of controlling dilution in a reactor. The divertor concept must be developed further to provide sufficient impurity control. A New Phase of JET will be undertaken to demonstrate effective methods of impurity control in an axisymmetric pumped divertor configuration.

The JET pumped divertor is an experiment to study impurity control scenarios and techniques in conditions relevant to the Next Step. For such an experiment, operational flexibility is essential. The design features four divertor coils which will permit experiments of a range of magnetic configurations. The targets are the most critical design issue and a two step approach will be followed for their installation and testing. It is expected that the JET pumped divertor experiment will yield essential data for the design of the divertor of a Next Step device.

## REFERENCES

- [1] The JET Project - Design Proposal: EUR-JET-R5;
- [2] Rebut, P-H, et al, Fusion Technology, **11**, (1987), 13-281;
- [3] Bickerton RJ and the JET Team, Proc. 12th Int. Conf. on Plasma Physics and Controlled Nuclear Fusion Research (Nice France), Nuclear Fusion Supplement, (1989) Vol.1, p41;
- [4] Dietz KJ, et al, Proc. 13th Symp. on Fusion Engineering (SOFE), (Knoxville, U.S.A., 1989) Vol.1, p512;
- [5] Rebut, P-H. et al, JET Contributions to the Workshop on the New Phase for JET: The Pumped Divertor Proposal (September 1989), JET Report - JET-R(89)16;
- [6] Keilhacker M, et al, Proc. 17th European Conf. on Controlled Fusion and Plasma Physics (Berlin, F.R.G., 1991), Plasma Physics and Controlled Fusion, **33** 1453 (1991)

**Table I**  
**JET Parameters**

<b>Parameters</b>	<b>Design Values</b>	<b>Achieved Values</b>
Plasma Major Radius ( $R_0$ )	2.96m	2.5-3.4m
Plasma Minor Radius horizontal (a)	1.25m	0.8-1.2m
Plasma Minor Radius vertical (b)	2.1m	0.8-2.1m
Toroidal Field at $R_0$	3.45T	3.45T
Plasma Current:		
Limiter mode	4.8MA	7.1MA
Single null X-point	not foreseen	5.1MA
Double null X-point	not foreseen	4.5MA
Neutral Beam Power		
(80kV, D)	20MW	21MW
(140kV, D)	15MW	15MW
Ion Cyclotron Resonance Heating Power to Plasma	15MW	22MW

**Table II**  
**Parameters of X-Point Plasmas**

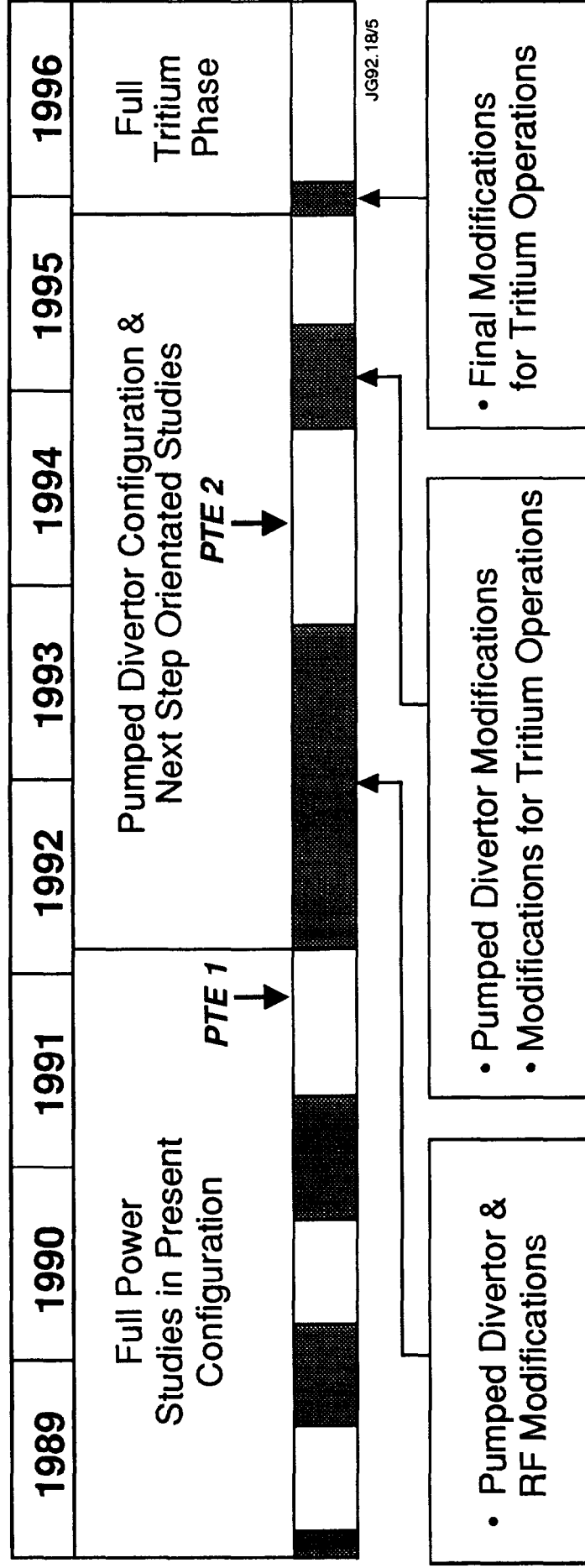
<b>Configuration</b>	<b>Fat</b>	<b>Slim</b>
Plasma current (MA)	6	5
Plasma volume (m <sup>3</sup> )	88	75
Connection length (m)	3.1	8.2
Safety factor $q_{95}$	2.2	2.4
Sum of divertor coil currents (MA <sub>t</sub> )	0.74	1.5

**Table III**  
**Diagnostics for the New Phase of JET**

<b>Diagnostic</b>	<b>Purpose</b>	<b>Status</b>
X-point bolometer	Time and space radiated power from X-point region	Commissioning
Divertor bolometer	Time and space resolved radiated power from divertor region	Design
Magnetic diagnostic for divertor	Identification of flux surface geometry	Design
Calorimetry for divertor	Poloidal temperature distribution on target	Design
Fast ion and alpha-particle diagnostic	Space and time resolved velocity distribution	Under construction
q-profile Thomson scattering	Measurement of q-profile	Under development
Lidar Thomson scattering	Higher spatial resolution, $n_e$ and $T_e$ in plasma edge	Design
Lidar Thomson scattering	$T_e$ and $n_e$ profile in divertor region	Design
High Energy neutral particle analyser	Ion energy distribution up to 3.5MeV	Under construction
X-point reflectometer	Peak $n_e$ in X-point	Under development
Microwave interferometer	$\int n_e ds$ in divertor region	Design
Microwave reflectometer	Peak $n_e$ in divertor region	Design
Compact soft X-ray cameras	MHD instabilities, plasma shape	Design
Compact soft X-ray camera	Toroidal mode number determination	Design
Electron cyclotron absorption	$n_e$ $T_e$ profile in divertor region	Design
Surface temperature	Surface temperature of target tiles	Commissioning
14MeV neutron spectrometer 14MeV time-of-flight neutron spectrometer	Neutron spectra in D-T discharges, ion temperatures and energy distributions	Under construction Awaiting installation
Bragg rotor X-ray spectrometer	Monitor of low and medium- Z impurity radiation	Design
Poloidal rotation	Multichannel spectroscopic measurement of poloidal rotation	Design
X-point target spectroscopy	Impurity and H-spectra spatially resolved	In preparation
Toroidal view	Flow velocity	Design
Periscopes	Impurity density in divertor	Design
VUV and XUV Spectroscopy	Impurity survey in the divertor region	Design
Fixed Langmuir probes for divertor	Plasma parameters at target	Design
Fast pressure gauges for divertor	Neutral particle fluxes on target	Design
Escaping alpha-particle detector	D-T alpha-particle confinement	Design



**Table IV**  
**JET Programme Schedule 1989–1996**



*PTE:* Preliminary Tritium Experiment

JM

INSTITUTE  
OF TECHNOLOGY

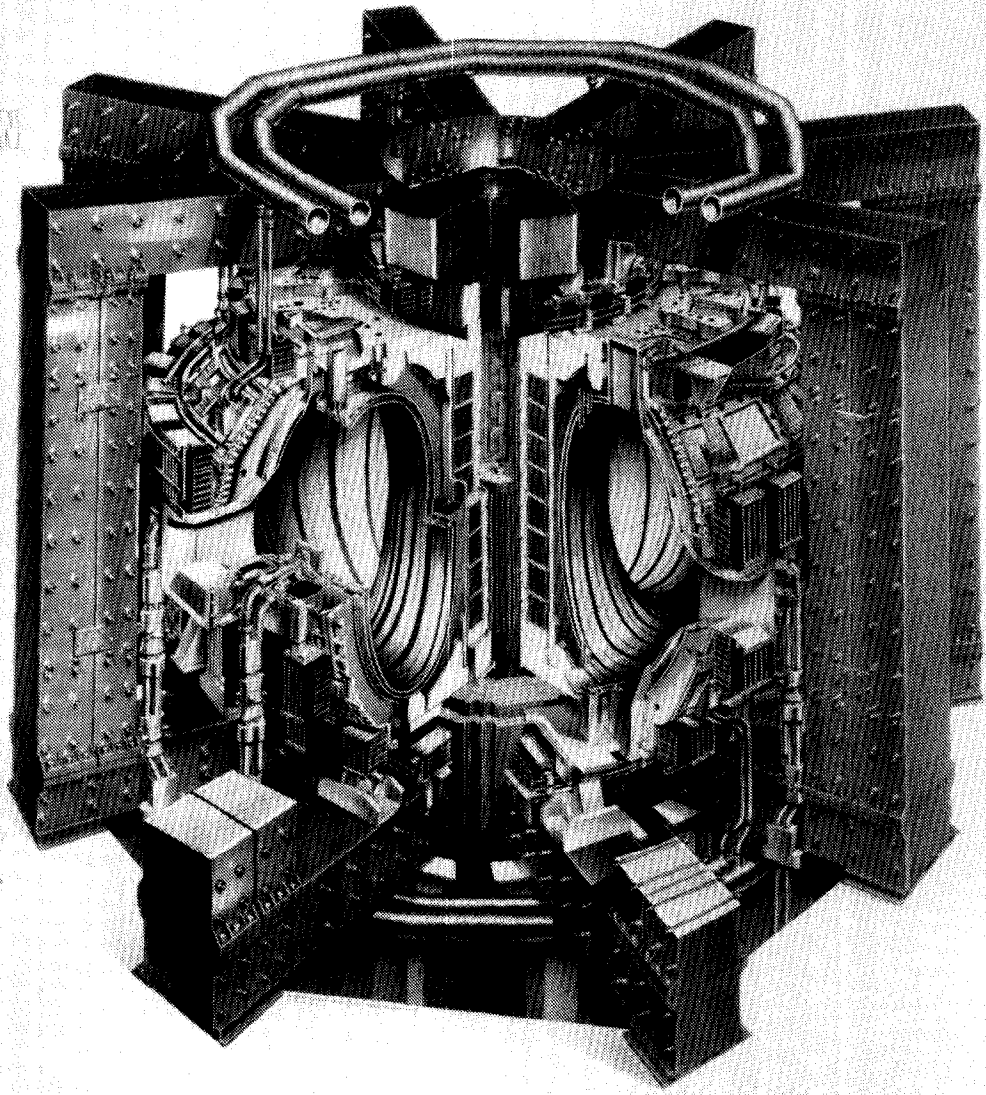


Fig.1: Schematic diagram of the JET machine.

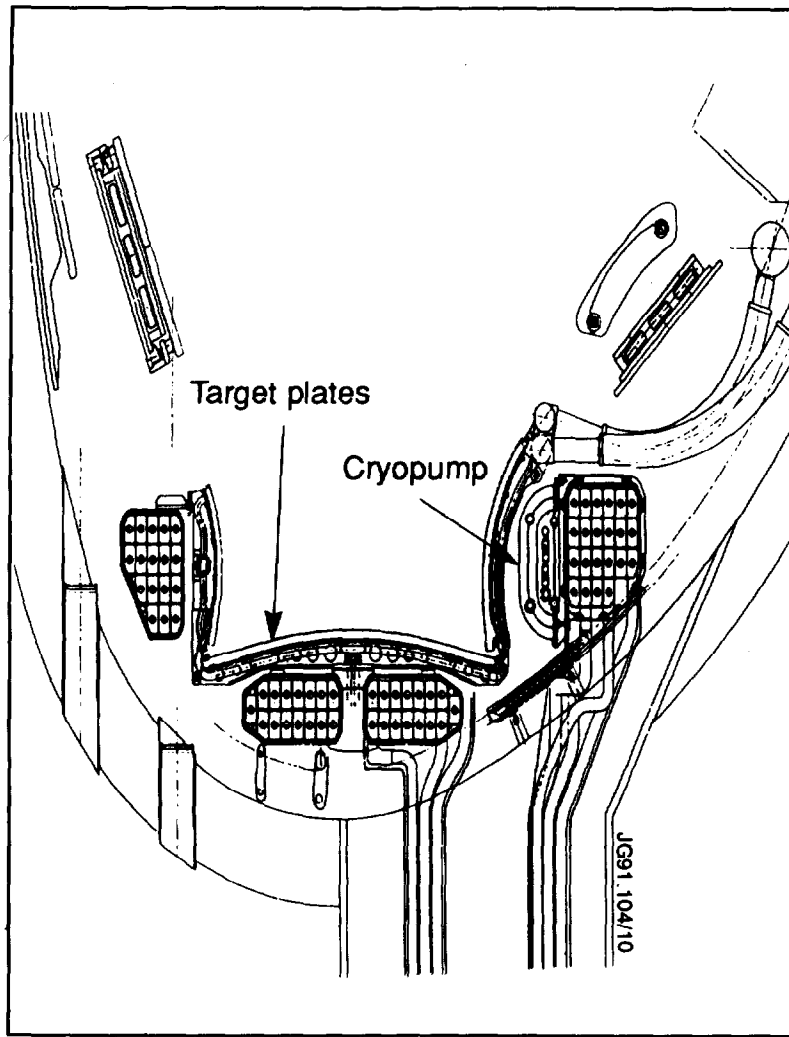


Fig.2: Schematic diagram of the JET pumped divertor.

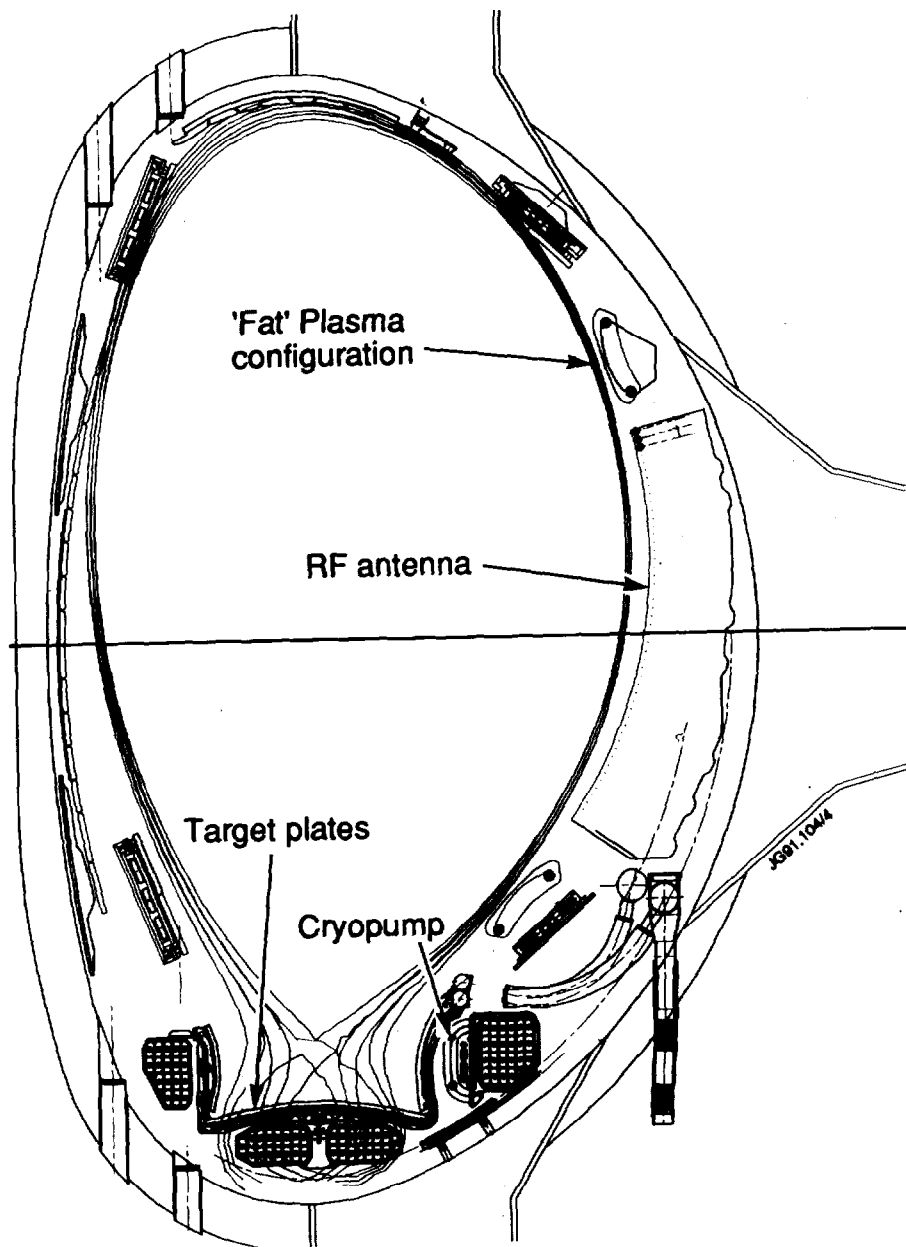


Fig.3: The JET pumped divertor configuration, in which the "fat" plasma has a moderate elongation and a short connection length.

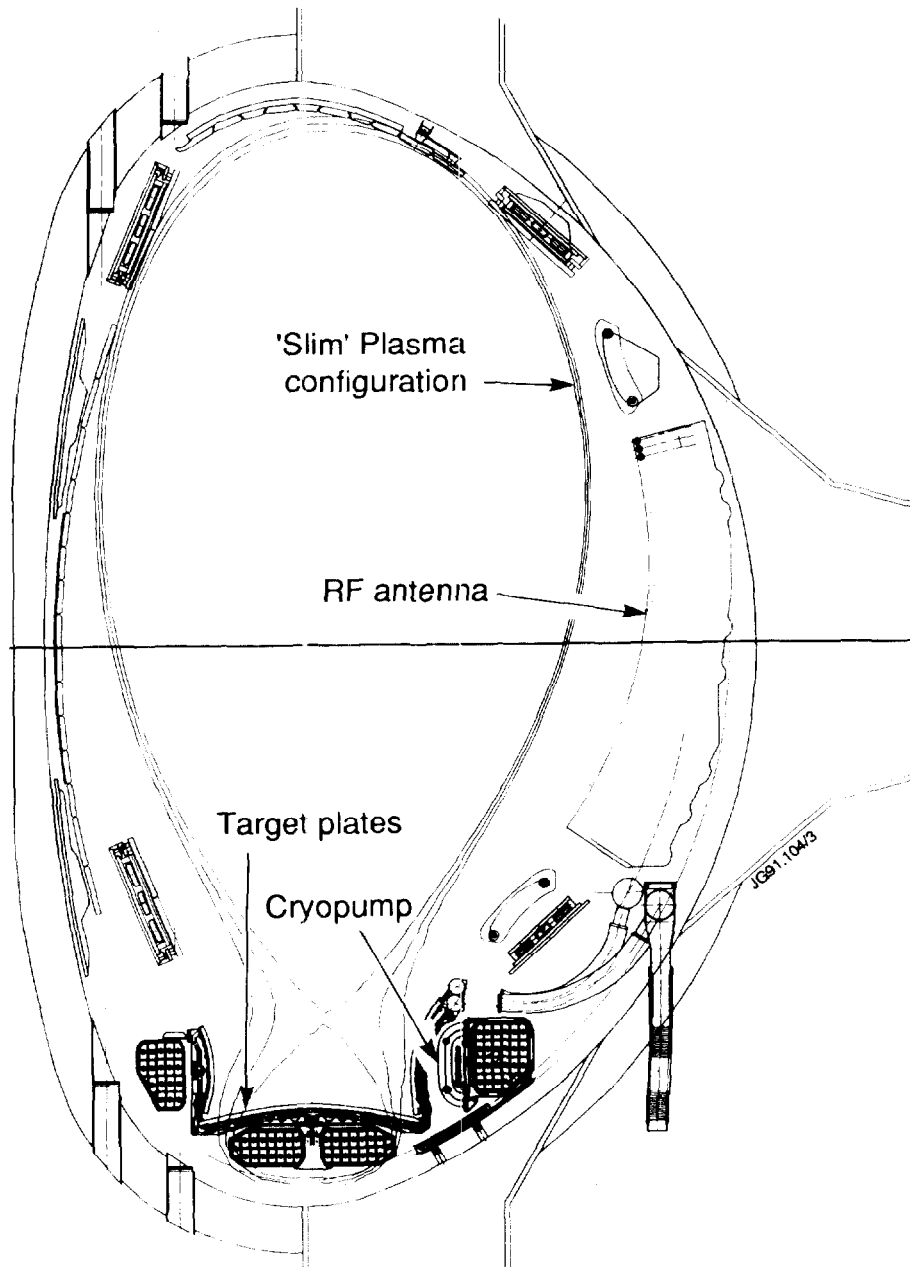


Fig.4: The JET pumped divertor configuration, in which the "slim" plasma is more elongated and has a longer connection length.

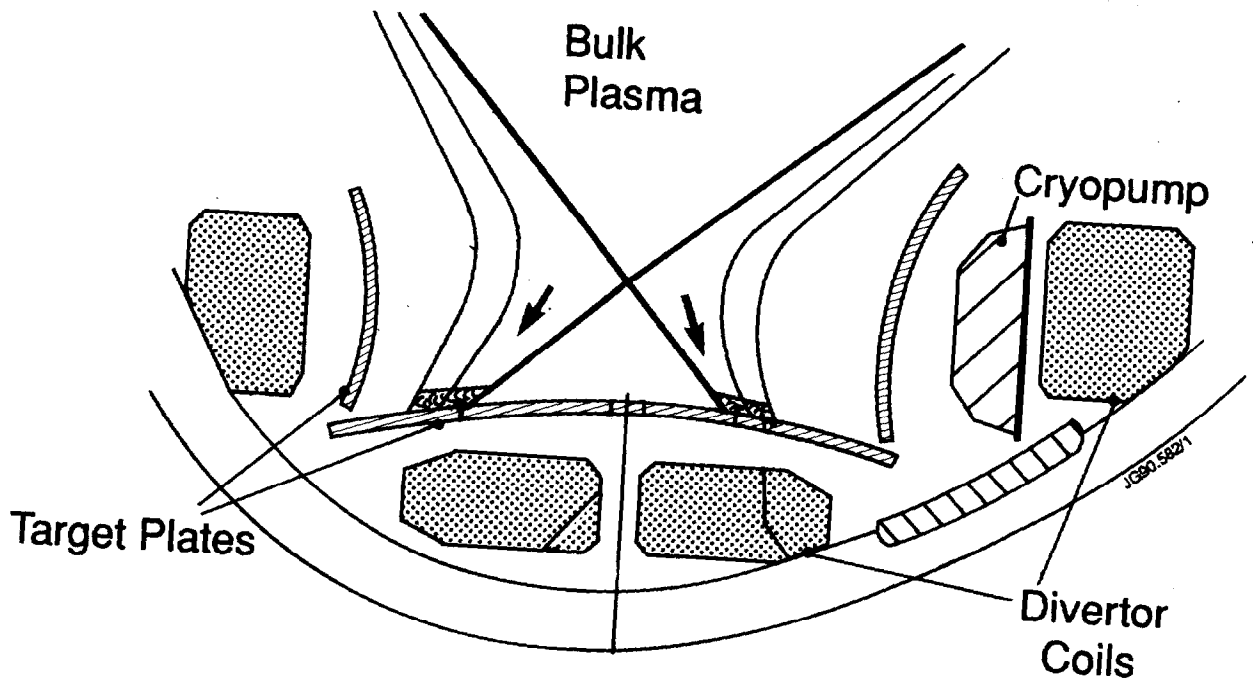


Fig.5: The components of the pumped divertor.

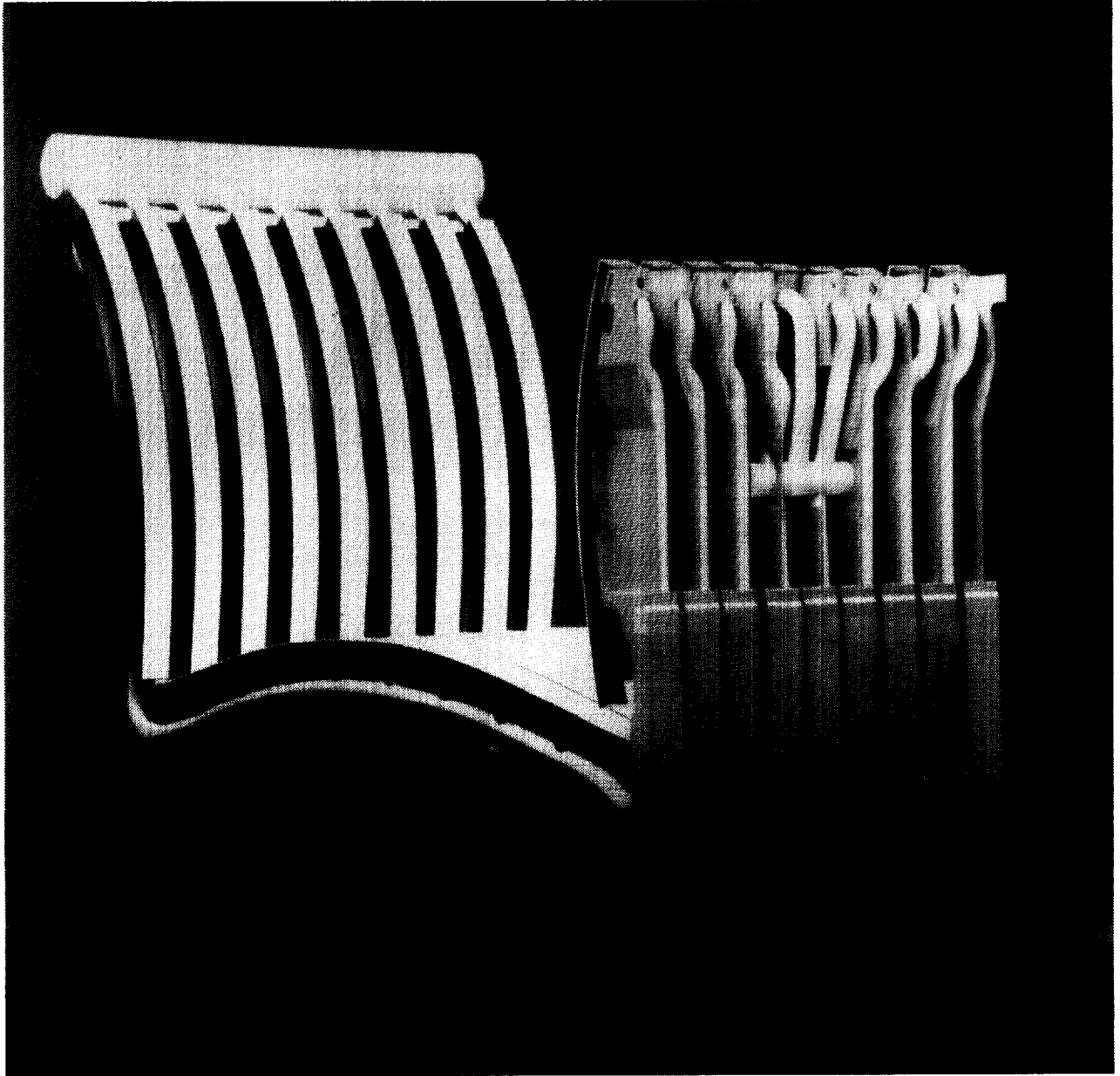


Fig.6: Layout of the targets.

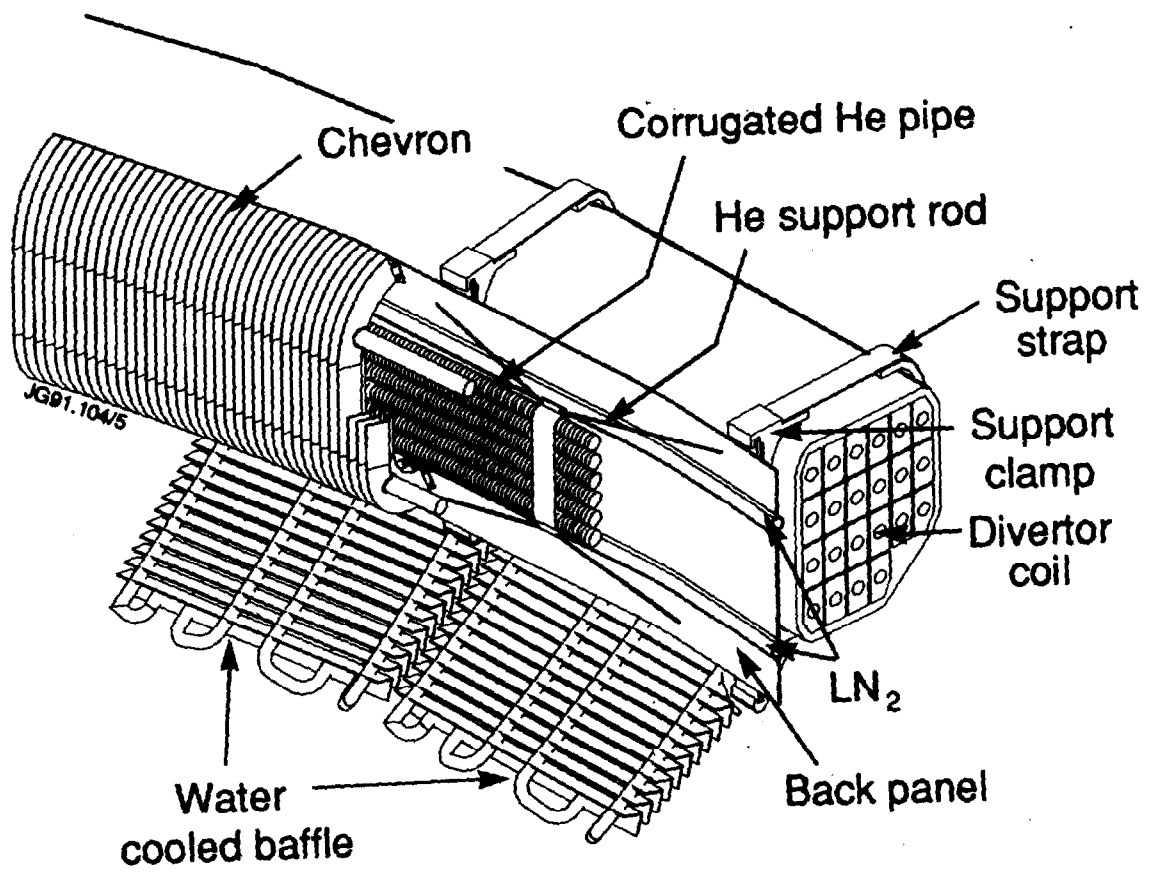
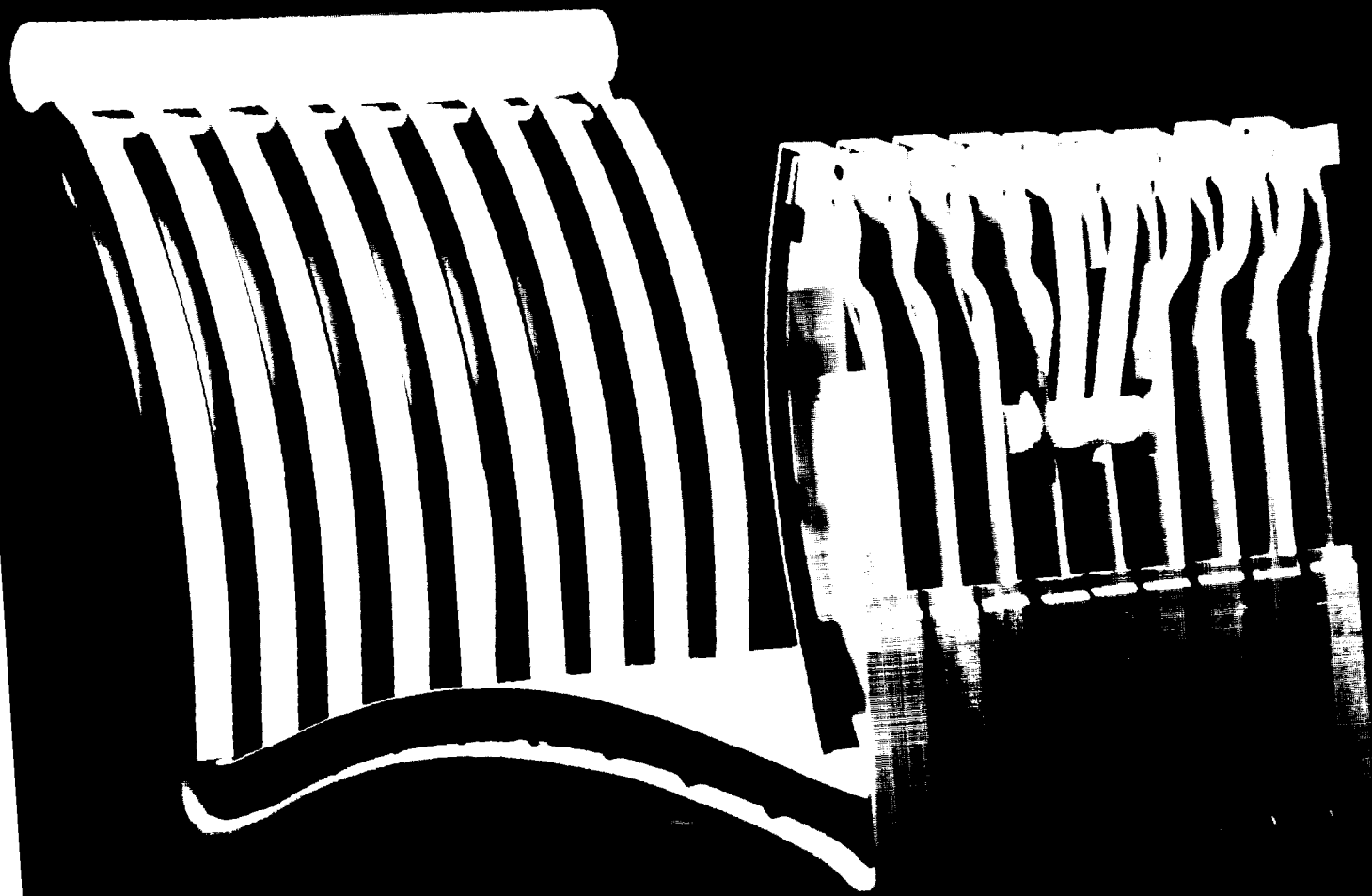
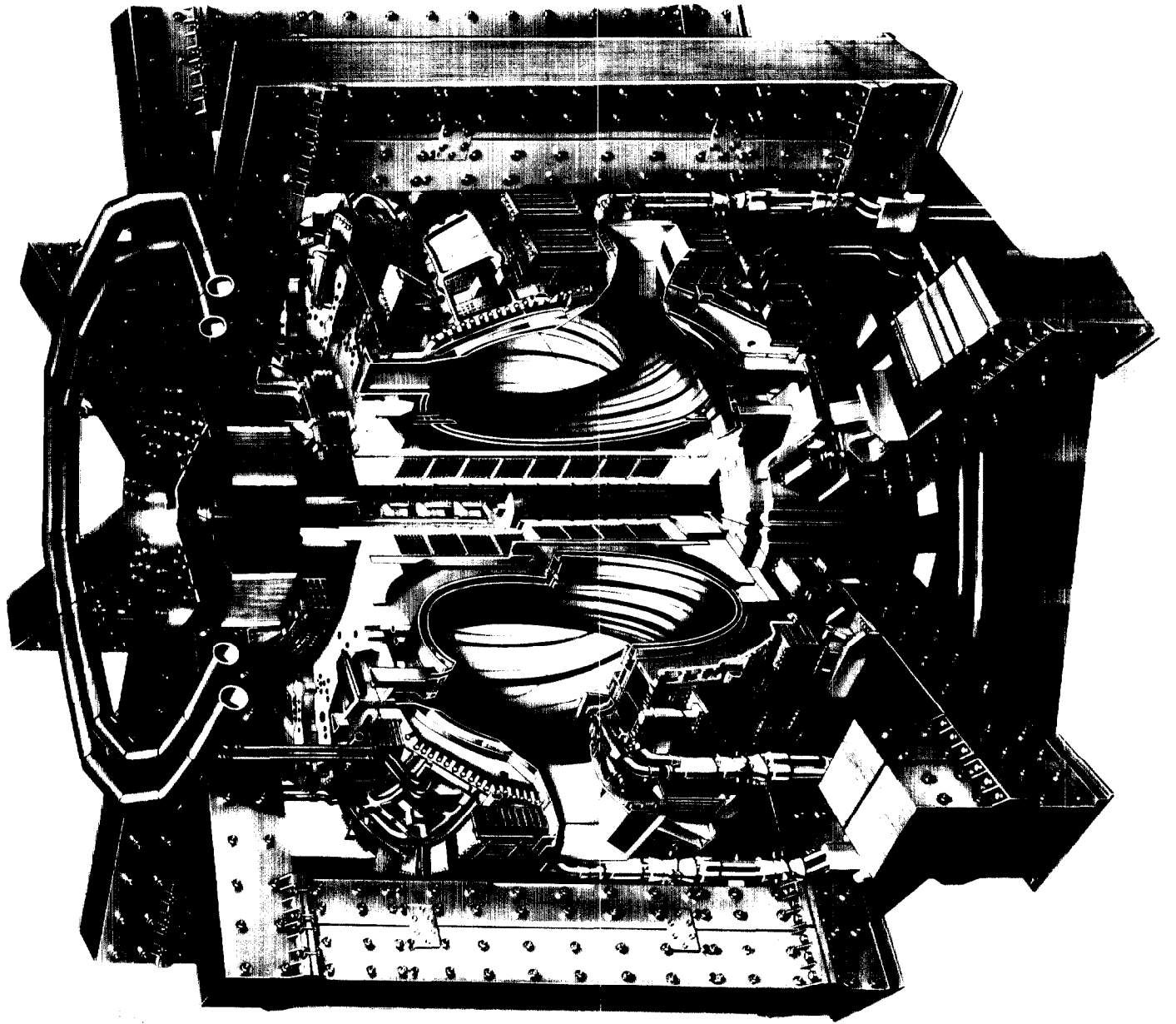


Fig.7: Layout of the cryopump.







— 157

## ANNEX

P.-H. REBUT, A. GIBSON, M. HUGUET, J.M. ADAMS<sup>1</sup>, B. ALPER, H. ALTMANN, A. ANDERSEN<sup>2</sup>, P. ANDREW<sup>3</sup>, M. ANGELONE<sup>4</sup>, S. ALI-ARSHAD, P. BAIGGER, W. BAILEY, B. BALET, P. BARABASCHI, P. BARKER, R. BARNESLEY<sup>5</sup>, M. BARONIAN, D.V. BARTLETT, L. BAYLOR<sup>6</sup>, A.C. BELL, G. BENALI, P. BERTOLDI, E. BERTOLINI, V. BHATNAGAR, A.J. BICKLEY, D. BINDER, H. BINDSLEV<sup>2</sup>, T. BONICELLI, S.J. BOOTH, G. BOSIA, M. BOTMAN, D. BOUCHER, P. BOUCQUEY, P. BREGER, H. BRELEN, H. BRINKSCHULTE, D. BROOKS, A. BROWN, T. BROWN, M. BRUSATI, S. BRYAN, J. BRZOZOWSKI<sup>7</sup>, R. BUCHSE<sup>22</sup>, T. BUDD, M. BURES, T. BUSINARO, P. BUTCHER, H. BUTTGEREIT, C. CALDWELL-NICHOLS, D.J. CAMPBELL, P. CARD, G. CELENTANO, C.D. CHALLIS, A.V. CHANKIN<sup>8</sup>, A. CHERUBINI, D. CHIRON, J. CHRISTIANSEN, P. CHUILON, R. CLAESEN, S. CLEMENT, E. CLIPSHAM, J.P. COAD, I.H. COFFEY<sup>9</sup>, A. COLTON, M. COMISKEY<sup>10</sup>, S. CONROY, M. COOKE, D. COOPER, S. COOPER, J.G. CORDEY, W. CORE, G. CORRIGAN, S. CORTI, A.E. COSTLEY, G. COTTRELL, M. COX<sup>11</sup>, P. CRIPWELL<sup>12</sup>, O. Da COSTA, J. DAVIES, N. DAVIES, H. de BLANK, H. de ESCH, L. de KOCK, E. DEKSNIS, F. DELVART, G.B. DENNE-HINNOV, G. DESCHAMPS, W.J. DICKSON<sup>13</sup>, K.J. DIETZ, S.L. DMITRENKO, M. DMITRIEVA<sup>14</sup>, J. DOBBING, A. DOGLIO, N. DOLGETTA, S.E. DORLING, P.G. DOYLE, D.F. DÜCHS, H. DUQUENOY, A. EDWARDS, J. EHRENBERG, A. EKEDAHL, T. ELEVANT<sup>7</sup>, S.K. ERENTS<sup>11</sup>, L.G. ERIKSSON, H. FAJEMIROKUN<sup>12</sup>, H. FALTER, J. FREILING<sup>15</sup>, F. FREVILLE, C. FROGER, P. FROISSARD, K. FULLARD, M. GADEBERG, A. GALETSAS, T. GALLAGHER, D. GAMBIER, M. GARRIBBA, P. GAZE, R. GIANNELLA, R.D. GILL, A. GIRARD, A. GONDHALEKAR, D. GOODALL<sup>11</sup>, C. GORMEZANO, N.A. GOTTARDI, C. GOWERS, B.J. GREEN, B. GRIEVSON, R. HAANGE, A. HAIGH, C.J. HANCOCK, P.J. HARBOUR, T. HARTRAMPF, N.C. HAWKES<sup>11</sup>, P. HAYNES<sup>11</sup>, J.L. HEMMERICH, T. HENDER<sup>11</sup>, J. HOEKZEMA, D. HOLLAND, M. HONE, L. HORTON, J. HOW, M. HUART, I. HUGHES, T.P. HUGHES<sup>10</sup>, M. HUGON, Y. HUO<sup>16</sup>, K. IDA<sup>17</sup>, B. INGRAM, M. IRVING, J. JACQUINOT, H. JAECKEL, J.F. JAEGER, G. JANESCHITZ, Z. JANKOVICZ<sup>18</sup>, O.N. JARVIS, F. JENSEN, E.M. JONES, H.D. JONES, L.P.D.F. JONES, S. JONES<sup>19</sup>, T.T.C. JONES, J.-F. JUNGER, F. JUNIQUE, A. KAYE, B.E. KEEN, M. KEILHACKER, G.J. KELLY, W. KERNER, A. KHUDOLEEV<sup>21</sup>, R. KONIG, A. KONSTANTELLOS, M. KOVANEN<sup>20</sup>, G. KRAMER<sup>15</sup>, P. KUPSCHUS, R. LÄSSER, J.R. LAST, B. LAUNDY, L. LAURO-TARONI, M. LAVEYRY, K. LAWSON<sup>11</sup>, M. LENNHOLM, J. LINGERTAT<sup>22</sup>, R.N. LITUNOVSKI, A. LOARTE, R. LOBEL, P. LOMAS, M. LOUGHLIN, C. LOWRY, J. LUPO, A.C. MAAS<sup>15</sup>, J. MACHUZAK<sup>19</sup>, B. MACKLIN, G. MADDISON<sup>11</sup>, C.F. MAGGI<sup>23</sup>, G. MAGYAR, W. MANDL<sup>22</sup>, V. MARCHESE, G. MARCON, F. MARCUS, J. MART, D. MARTIN, E. MARTIN, R. MARTIN-SOLIS<sup>24</sup>, P. MASSMANN, G. MATTHEWS, H. McBRYAN, G. McCRACKEN<sup>11</sup>, J. McKIVITT, P. MERIGUET, P. MIELE, A. MILLER, J. MILLS, S.F. MILLS, P. MILLWARD, P. MILVERTON, E. MINARDI<sup>4</sup>, R. MOHANTI<sup>25</sup>, P.L. MONDINO, D. MONTGOMERY<sup>26</sup>, A. MONTVAI<sup>27</sup>, P. MORGAN, H. MORSI, D. MUIR, G. MURPHY, R. MYRNÄS<sup>28</sup>, F. NAVE<sup>29</sup>, G. NEWBERT, M. NEWMAN, P. NIELSEN, P. NOLL, W. OBERT, D. O'BRIEN, J. ORCHARD, J. O'ROURKE, R. OSTROM, M. OTTAVIANI, M. PAIN, F. PAOLETTI, S. PAPASTERGIOU, W. PARSONS, D. PASINI, D. PATEL, A. PEACOCK, N. PEACOCK<sup>11</sup>, R.J.M. PEARCE, D. PEARSON<sup>12</sup>, J.F. PENG<sup>16</sup>, R. PEPE DE SILVA, G. PERINIC, C. PERRY, M. PETROV<sup>21</sup>, M.A. PICK, J. PLANCOULAINE, J.-P. POFFÉ, R. PÖHLCHEN, F. PORCELLI, L. PORTE<sup>13</sup>, R. PRENTICE, S. PUPPIN, S. PUTVINSKII<sup>8</sup>, G. RADFORD<sup>30</sup>, T. RAIMONDI, M.C. RAMOS DE ANDRADE, R. REICHLER, J. REID, S. RICHARDS, E. RIGHI, F. RIMINI, D. ROBINSON<sup>11</sup>, A. ROLFE, R.T. ROSS, L. ROSSI, R. RUSS, P. RUTTER, H.C. SACK, G. SADLER, G. SAIBENE, J.L. SALANAVE, G. SANAZZARO, A. SANTAGIUSTINA, R. SARTORI, C. SBORCHIA, P. SCHILD, M. SCHMID, G. SCHMIDT<sup>31</sup>, B. SCHUNKE, S.M. SCOTT, L. SERIO, A. SIBLEY, R. SIMONINI, A.C.C. SIPS, P. SMEULDERS, R. SMITH, R. STAGG, M. STAMP, P. STANGEBY<sup>3</sup>, R. STANKIEWICZ<sup>32</sup>, D.F. START, C.A. STEED, D. STORK, P.E. STOTT, P. STUBBERFIELD, D. SUMMERS, H. SUMMERS<sup>13</sup>, L. SVENSSON, J.A. TAGLE<sup>33</sup>, M. TALBOT, A. TANGA, A. TARONI, C. TERELLA, A. TERRINGTON, A. TESINI, P.R. THOMAS, E. THOMPSON, K. THOMSEN, F. TIBONE, A. TISCORNIA, P. TREVALION, B. TUBBING, P. VAN BELLE, H. VAN DER BEKEN, G. VLASES, M. VON HELLERMANN, T. WADE, C. WALKER, R. WALTON<sup>31</sup>, D. WARD, M.L. WATKINS, N. WATKINS, M.J. WATSON, S. WEBER<sup>34</sup>, J. WESSON, T.J. WIJNANDS, J. WILKS, D. WILSON, T. WINKEL, R. WOLF, D. WONG, C. WOODWARD, Y. WU<sup>35</sup>, M. WYKES, D. YOUNG, I.D. YOUNG, L. ZANNELLI, A. ZOLFAGHARI<sup>19</sup>, W. ZWINGMANN

- 
- <sup>1</sup> Harwell Laboratory, UKAEA, Harwell, Didcot, Oxfordshire, UK.
  - <sup>2</sup> Risø National Laboratory, Roskilde, Denmark.
  - <sup>3</sup> Institute for Aerospace Studies, University of Toronto, Downsview, Ontario, Canada.
  - <sup>4</sup> ENEA Frascati Energy Research Centre, Frascati, Rome, Italy.
  - <sup>5</sup> University of Leicester, Leicester, UK.
  - <sup>6</sup> Oak Ridge National Laboratory, Oak Ridge, TN, USA.
  - <sup>7</sup> Royal Institute of Technology, Stockholm, Sweden.
  - <sup>8</sup> I.V. Kurchatov Institute of Atomic Energy, Moscow, Russian Federation.
  - <sup>9</sup> Queens University, Belfast, UK.
  - <sup>10</sup> University of Essex, Colchester, UK.
  - <sup>11</sup> Culham Laboratory, UKAEA, Abingdon, Oxfordshire, UK.
  - <sup>12</sup> Imperial College of Science, Technology and Medicine, University of London, London, UK.
  - <sup>13</sup> University of Strathclyde, Glasgow, UK.
  - <sup>14</sup> Keldysh Institute of Applied Mathematics, Moscow, Russian Federation.
  - <sup>15</sup> FOM-Institute for Plasma Physics "Rijnhuizen", Nieuwegein, Netherlands.
  - <sup>16</sup> Institute of Plasma Physics, Academia Sinica, Hefei, Anhui Province, China.
  - <sup>17</sup> National Institute for Fusion Science, Nagoya, Japan.
  - <sup>18</sup> Soltan Institute for Nuclear Studies, Otwock/Świerk, Poland.
  - <sup>19</sup> Plasma Fusion Center, Massachusetts Institute of Technology, Boston, MA, USA.
  - <sup>20</sup> Nuclear Engineering Laboratory, Lappeenranta University, Finland.
  - <sup>21</sup> A.F. Ioffe Physico-Technical Institute, St. Petersburg, Russian Federation.
  - <sup>22</sup> Max-Planck-Institut für Plasmaphysik, Garching, Germany.
  - <sup>23</sup> Department of Physics, University of Milan, Milan, Italy.
  - <sup>24</sup> Universidad Complutense de Madrid, Madrid, Spain.
  - <sup>25</sup> North Carolina State University, Raleigh, NC, USA.
  - <sup>26</sup> Dartmouth College, Hanover, NH, USA.
  - <sup>27</sup> Central Research Institute for Physics, Budapest, Hungary.
  - <sup>28</sup> University of Lund, Lund, Sweden.
  - <sup>29</sup> Laboratório Nacional de Engenharia e Tecnologia Industrial, Sacavem, Portugal.
  - <sup>30</sup> Institute of Mathematics, University of Oxford, Oxford, UK.
  - <sup>31</sup> Princeton Plasma Physics Laboratory, Princeton University, Princeton, NJ, USA.
  - <sup>32</sup> RCC Cyfronet, Otwock/Świerk, Poland.
  - <sup>33</sup> Centro de Investigaciones Energéticas, Medioambientales y Tecnológicas, Madrid, Spain.
  - <sup>34</sup> Freie Universität, Berlin, Germany.
  - <sup>35</sup> Institute for Mechanics, Academia Sinica, Beijing, China.